Iran University of Science and Technology

International Journal of Automotive Engineering

Journal Homepage: ijae.iust.ac.ir

ISSN: 2008-9899

Comparative lifecycle assessment of diesel, hydrogen and electric buses in real driving cycles in Tehran

Hossein Gharaei, Pouria Ahmadi*, Mehdi Ashjaee

[1]School of Mechanical Engineering, College of Engineering, University of Tehran, PO. Box 11155-4563, Tehran, Iran

ARTICLE INFO

Article history:

Received: 1 May 2020

Accepted: 30 May 2020

Published: 1 June 2020

Keywords:

Fuel consumption

Real driving condition

Life cycle assessment

PEM fuel-cell

Longitudinal vehicle dynamics

ABSTRACT

This study uses real driving cycles of a city bus and a standard driving cycle "WLTP" to implement a full comparison for energy demand and fuel consumption for different propulsion systems (i.e., Diesel ICE, Fuel cell and Electric engines). These results were obtained by simulating each propulsion system in MATLAB, SIMULINK and EES. To better understand the comparison, a life cycle assessment is conducted using "GREET" and "GHGenius" software, which represents a clear demonstration of side effects and emissions of each engine on the environment. The results show that for "WLTP" cycle the bus needs 2423kJ energy for traveling each kilometer while the averaged amount of energy for traveling one kilometer of real driving cycle reaches to 1708kJ, the difference is due to speed range difference and number of stop/start points. In both cycles inertia force consumes the most used energy portion of the bus. By computing total energy use of an electric bus we conclude, electric buses use almost 58% of electric energy for driving and the rest is lost. Then fuel cell and internal combustion engine buses have energy efficiency of 36% and 24% respectively. Concerning LCA analysis, it becomes apparent that unlike efficiency, electric buses are not environmentally benign as fuel cell buses. LCA analysis showed that fuel cell buses that use steam reforming hydrogen production process are a cleaner option than electric buses, for instance a fuel cell bus emit 90 (g/100km) CO, 140 (g/100km) SOx and 67 (g/100km) NOx while an electric bus emit 110 (g/100km), 220 (g/100km) and 99 (g/100km) respectively which in all cases the fuel cell bus is more environment friendly than the electric bus. Finally, since diesel buses produce the most emission, especially CO2, and consume the most energy in the total life cycle, they have no advantage for public transportation fleet.

1. Introduction

The major concerns that human face nowadays can be summarized in two subjects, energy, and environment. According to Suganthi et. al [1] energy consumption during the last decade has increased drastically, so energy management is crucial for future economic prosperity and environmental security, as it is evident, transportation accounts for about 30% of the total global GHG emission. Reducing emissions from transportation requires substantial efforts from various disciplines. Reducing the weight of vehicles, improving the efficiency of vehicles, reducing the driving dependency, switching to more environmentally benign fuels, and using

*Corresponding Author
Email Address: pahmadi@ut.ac.ir
https://doi.org/10.22068/ase.2020.542

[DOI: 10.22068/ase.2020.542]

improving public transportation could be some of the potential options to mitigate the emissions [2,3]. Lajunen et. al [4] discussed energy consumption and emission of city buses in fleet operation. Their research included two parallel, two series hybrid and one electric city bus and the results showed that plug-in hybrid and electric buses performed the best in terms of energy consumption and emissions. Vepsäläinen et. al [5], in another research, studied the energy demand of electric city buses, The uncertainty of operating conditions such as weather and payload caused variations in the bus energy demand. To predict the energy demand, the writer composed a computationally efficient model that is required for real-time applications. To indicate the importance of using real driving cycles, Gallet et al. [6] used several state-of-the-art approaches to determine the energy requirement of electric buses that use individual-specific energy demand values. Local bus route characteristics, is more beneficial and inclusive than standard cycles. So, their research is done based on the standard driving cycles. In this research we did so and in order to have a realistic conclusion, real driving patterns that there is a chance of occurring any unexpected events or mechanical problems is considered. To decide for the superior fleet, it is needed not only to discuss just one propulsion system but also busses with different engines should be examined. Cubito et. al [7] did almost the same study but it was concluded that the effectiveness of hybrid electric buses strongly depends on energy management and power train efficiency. Also, it was mentioned that real-life results were much closer to worldwide harmonized light-duty test procedures (WLTP) than the new European driving cycle. This study can be implemented as a realistic way of analyzing the impact of different driving cycles and operating conditions on energy demand and CO_2 emissions through the limited information available from chassis dyno tests.

The other alternative solution which has attracted much attention is using hydrogen as an alternative fuel. There are several studies that considered fuel cells for light-duty vehicles [8–10] from various point of view. Gao et. al [11] employed an energy management strategy to control the power flow of a fuel cell hybrid power train to overcome fuel cell drawbacks such as no regenerative energy recovery during braking, and slow response of fuel cell vehicles. Fontaras et. al [12] used both real and legislated driving cycles to compare emissions of different fuels and compare real driving cycle results to standard driving cycles.

Another factor in deciding premier and the cleanest fleet, is to calculate the environmental impacts of all processes which include from the beginning of the product (i.e., fuel production) to vehicle assembly and disposal. A tool that can do this is called life cycle assessment. LCA methods consist of different approaches, for instance considering fuel life cycle, vehicle life cycle, operating life cycle or total life cycle will lead to various results, these variations can be explained by figure 1.

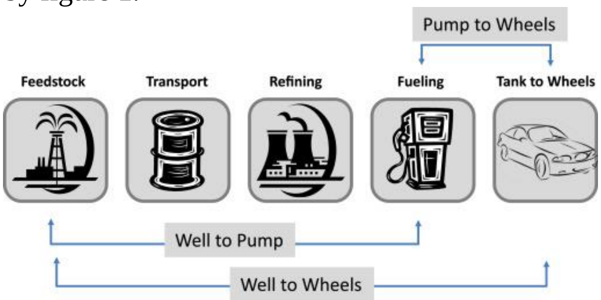

Figure 1:Different LCA methods[1]

According to Jonker et. al [13] calculating lifetime environmental impact is a multi-step procedure, and its complete analysis consists of raw material acquisition, transportation, and processing, as well as product manufacturing, distribution, use, and disposal (or recycling process). LCA of fuel production is known as fuel-cycle analysis or WTP analysis (if the fuel is consumed in transportation applications, it is considered as WTW), while LCA of vehicle manufacturing is known as vehicle-cycle analysis. Correa et. al [14] did so and found that electric vehicles are markedly superior in the tank to wheel step, nevertheless actions should be done to generate and store electric energy with lower environmental effect. Ally et. al [15] performed the LCA analysis for buses with three different power sources, including a hydrogen fuel-cell bus. The lifecycle assessment of the fuel cell bus in this study determines the overall environmental footprint and energy demand, by studying all phases of the transportation system, including the hydrogen infrastructure, bus manufacturing, operation, and end-of-life disposal. The LCAs of the existing diesel and natural gas transportation systems developed in parallel. Ahmadi et al. [16] studied the fuel consumption and life cycle assessment of a fuel cell vehicle. In their study, the effects of fuel cell degradation and vehicle regenerative braking on the lifecycle metrics of the vehicle were investigated. The results showed that fuel cell degradation has a significant effect

1 https://www.sciencedirect.com/science/article/pii/S0360544214008573

on the vehicle fuel economy, which eventually results in a reduction of 21% in the fuel economy. As Granovskii et al. [17] studied, it is a need to compare different power sources to achieve reliable results. They compared vehicles running by gasoline ICE and hydrogen fuel cell and the results indicate that, when taking into account fossil fuel energy consumption and greenhouse gas emissions, the efficiency of the fuel cell vehicle employing hydrogen from natural gas should be at least 25-30% higher than a gasoline one, and only in this way, they could be considered competitive.

2. Method

2.1. Real driving pattern data acquisition

There are many researches that use every-day driving condition in order to achieve realistic results [6,18], for using real driving cycle in this study "speedometer GPS" app was used to record velocity, altitude, and geographical location of city buses during their ride. These data were recorded in Tehran and totally, more than 80 sets of data gathered in four different routes, one set of this data record which consist of bus driving route, speed and elevation profile are demonstrated in figure 3 and 4. To overcome human and GPS errors in data acquisition process, inaccurate data corrected by plotting the drive pattern and making minor changes to bus stop locations. To achieve realistic, practical, and comprehensive driving patterns, the writer used four different routes, which include city traffic, cruising area, altitude difference and sudden acceleration and deceleration which are characteristics of real driving nature. A set of data records is available in Fig 2,3 and 4.

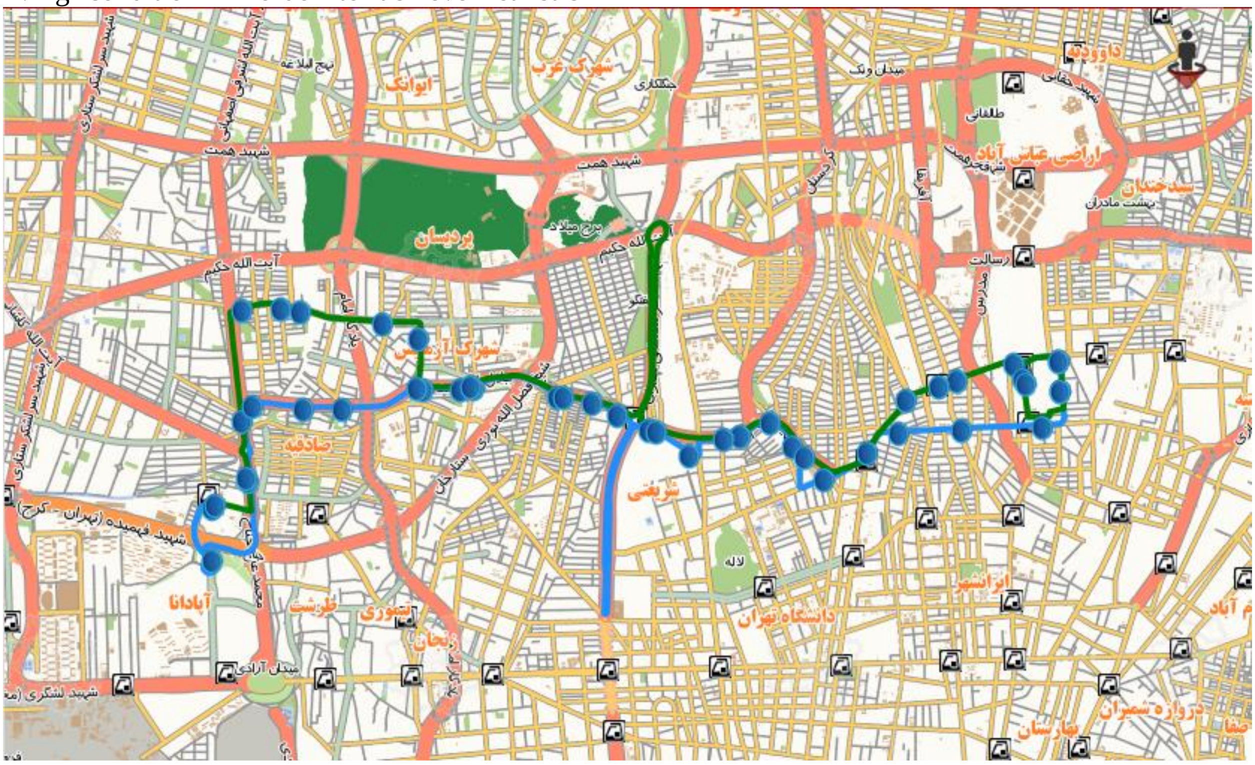

Figure 2:East-west route of real driving cycle records including bus stations

[DOI: 10.22068/ase.2020.542]

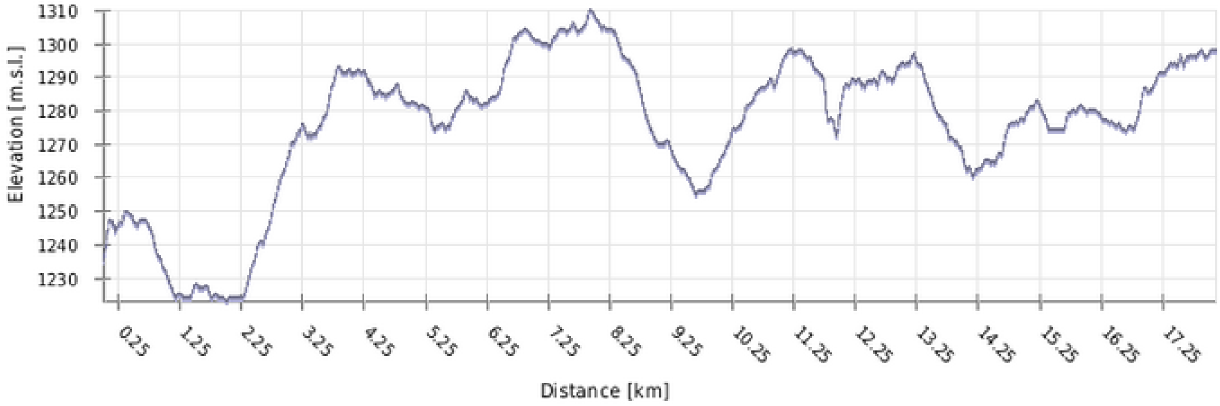

Figure 3:Elevation profile as a function of distance travelled in one set of recorded real driving cycles

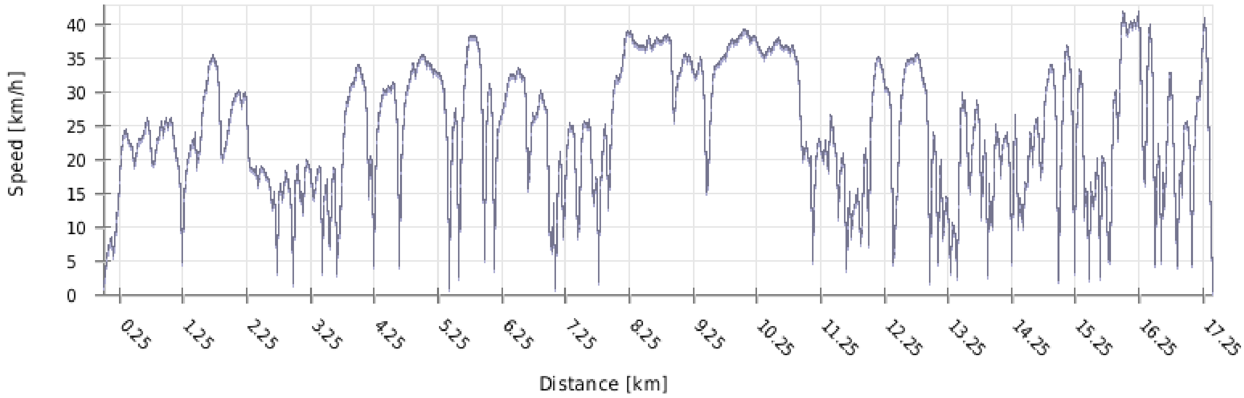

Figure 4:Speed profile of one set of recorded driving cycles

2.2. Vehicle dynamic model

The first step in modeling buses with different propulsion systems is to attain the energy demand of each driving cycle. The longitudinal model of a bus is used to calculate the energy demand since IC vehicles do not benefit from the regenerative braking system, just the acceleration and gradeability of a vehicle is simulated in this model. In electric and fuel cell buses, regenerative braking is used, so in addition to acceleration and gradeability, the regenerative braking energy source is simulated too.

For the simulation, some dynamic relations are used, which are presented below [19] these formulas simulated in MATLAB/SIMULINK in order to obtain energy consumption.

$$T_C = T_e - I_e\alpha_e \tag{1}$$

$$T_d = (T_c - I_T\alpha_e) \times N_T \tag{2}$$

$$T_a = F_x r + I_w\alpha_w = (T_d - I_d\alpha_d) \times N_{dif} \tag{3}$$

$$\alpha_d = N_{dif}\alpha_w \tag{4}$$

$$\alpha_c = N_T\alpha_d = N_T N_{dif}\alpha_w \tag{5}$$

$$F_x = \frac{(T_e \times N_{T,dif\times}\eta_{T,dif})}{r} - \{(I_e + I_T)N_{T,dif}^2 + I_d N_f^2 + I_w\}\frac{a_x}{r^2} \tag{6}$$

$$D_A = \frac{1}{2}C_D\rho V^2 A \tag{7}$$

$$R_x = C_R M g cos\theta \tag{8}$$

$$C_R = (0.0041 + 0.0000018 \times V)C_h \tag{9}$$

$$C_h = 1.5\ (for\ worn\ asphalt) \tag{10}$$

$$M \times a_x = F_x - R_x - D_A - R_{hx} - W \times sin\theta \tag{11}$$

$$\rightarrow (M+M_r)a_x = \frac{(T_e \times N_{T,dif} \times \eta_{T,dif})}{r} - Mg\cos\theta\big((0.0041 + 0.0000018 \times V)1.5\big) - \frac{1}{2}C_D\rho V^2 A - R_{hx} - W\sin\theta \quad (12)$$

$$M_r = \frac{(I_e + I_T)N_{T,dif}^2 + I_d N_f^2 + I_w}{r^2} \quad (13)$$

By using these formulas in the backward modeling approach, there is no need to model driver, and it directly uses velocity versus time data to obtain required torque and, therefore, energy demand of the vehicle in each cycle.

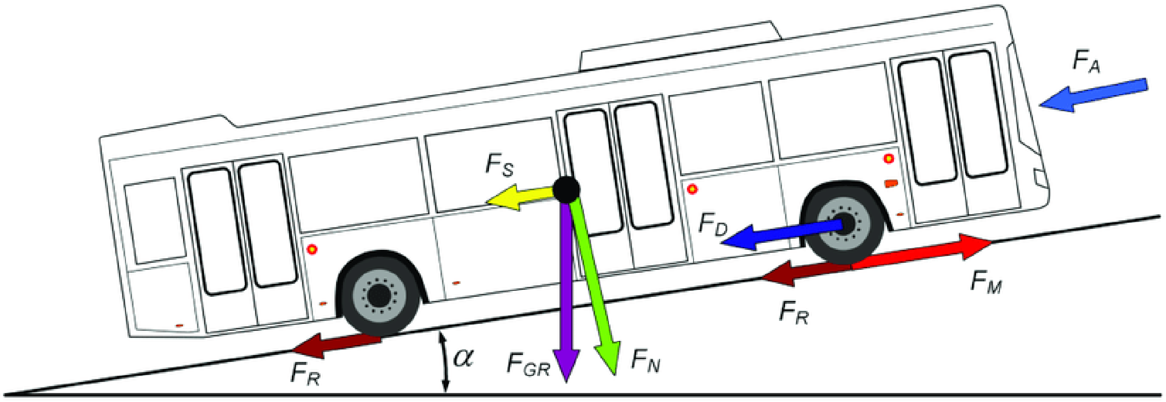

Figure 5:Bus longitudinal dynamic model schematic

2.3. Internal combustion engine

Internal combustion engine modeled in this research is a diesel engine (i.e., diesel fuel chemical formula is $C_{12}H_{23}$), this fuel has higher and lower heating values of 45.6 and 42.6 (MJ/kg) respectively. In this model, the combustion takes place with stoichiometric fuel/air ratio, so the chemical combustion equation is [20,21]:

$$C_{12}H_{23}(g) + 17.75(O_2 + 3.76N_2) \rightarrow 11.5H_2O(g) + 12CO_2(g) + 66.74N_2(g) + 7114kj \quad (14)$$

The conventional diesel engine in this research is assumed to have an energy efficiency of 35 percent and it works in ambient condition (298k for temperature and 101.325kPa for pressure).

2.4. PEM fuel cell

Proton-exchange membrane fuel cell is a type of fuel cell, being developed mainly for transport applications. Its distinguishing feature is low temperature and pressure range (50 to 100 °C). The governing reactions taking place in a conventional PEMFC is as follow:

$$anode\ reaction: \quad 2H_2 \rightarrow 4H^+ + 4e^- \quad (15)$$

$$cathode\ rection: \quad O_2 + 4H^+ + 4e^- \rightarrow 2H_2O \quad (16)$$

$$overall\ reaction: \quad 2H_2 + O_2 \rightarrow H_2O \quad (17)$$

2.4.1. Thermodynamic modeling of PEMFC

In a PEM fuel cell, actual cell potential $E(i)$ is lower than equilibrium potential (E_{Nernst}) due to irreversible losses, when the current flows is in the circuit, a departure from the thermodynamic potential occurs corresponding to the cell electrical work [22–24]. This departure is called overpotential (η), and it mainly consists of three different terms, activation, ohmic and concentration overpotential.

So, the net voltage of a single cell is expressed as[25–27]:

$$E(i) = E_{Nernst} + \eta_{act} + \eta_{ohmic} + \eta_{conc} \quad (18)$$

Nernst equation (or reversible voltage) of water electrolysis reaction is:

$$E_{Nernst} = 1.229 - 8.5 \times 10^{-4}(T - 298.15) + 4.3085 \times 10^{-5}T\{\ln(p^*_{H_2}) + 0.5\ln(p^*_{O_2})\} \quad (19)$$

Where $p^*_{H_2}$ and $p^*_{O_2}$ are the hydrogen and oxygen partial gas pressure at anode and cathode, respectively and they are calculated as:

[DOI: 10.22068/ase.2020.542]

$$p^*_{H_2} = \left(0.5 p^{sat}_{H_2O}\right)\left[\frac{1}{\exp\left(\frac{1.653i}{T^{1.334}}\right) x^{sat}_{H_2O}} - 1\right] \quad (20)$$

$$p^*_{O_2} = P\left[1 - x^{sat}_{H_2O} - x^{channel}_{other\ gases} e^{0.29i/T^{0.832}}\right] \quad (21)$$

Here $x^{sat}_{H_2O}$ is the molar fraction of water in the gas stream at saturation for specified temperature, and $x^{channel}_{other\ gases}$ is the molar fraction of other gases (except oxygen) in the air stream, they are described according to the formulas below:

$$x^{sat}_{H_2O} = \frac{P^{sat}_{H_2O}}{P} \quad (22)$$

$$x^{channel}_{other\ gases} = \frac{x^{in,hum}_{other\ gases} - x^{out,hum}_{other\ gases}}{\ln\left[\frac{x^{in,hum}_{other\ gases}}{x^{out,hum}_{other\ gases}}\right]} \quad (23)$$

Where

$$\log\left(P^{sat}_{H_2O}\right) = -2.1794 + 0.2953(T - 273.15) - (9.183 \times 10^{-5}) \times (T - 273.15)^2 + (1.454 \times 10^{-7})(T - 273.15)^3 \quad (24)$$

$$x^{in,hum}_{other\ gases} = 0.79(1 - x^{sat}_{H_2O}) \quad (25)$$

$$x^{out,hum}_{other\ gases} = \frac{1 - x^{sat}_{H_2O}}{1 + ((\lambda_{air} + 1)/\lambda_{air})(0.21/0.79)} \quad (26)$$

Activation overpotential is calculated by an empirical expression as [28]:

$$\eta_{act} = \beta_1 + \beta_2 T + \beta_3 T ln\left(C^{interface}_{O_2}\right) + \beta_4 T ln(I) \quad (27)$$

$$\beta_1 = -0.9514,\ \ \beta_2 = 3.12 \times 10^3$$
$$\beta_3 = 7.4 \times 10^{-5},\ \ \beta_4 = -1.87 \times 10^{-4}$$

Where

$$C^{interface}_{O_2} = \frac{P^*_{O_2}}{5.08 \times 10^6 \exp(-498/T)} \quad (28)$$

For calculating ohmic overpotential, we can employ ohm's law, as:

$$\eta_{ohmic} = -iR_{internal} \quad (29)$$

The internal resistance ($R_{internal}$) is calculated using the general equation:

$$R_{internal} = \frac{r_m L_m}{A_{cell}} \quad (30)$$

"r_m" is Nafion membrane specific resistivity, and it is proposed according to the experimental relation given as:

$$r_m = \frac{181.6\left[1 + 0.03(i) + 0.062\left(\frac{T}{303}\right)^2 i^{2.5}\right]}{[13.366 - 3i]\exp(4.18(T - 303/T))} \quad (31)$$

Concentration losses occur in both electrodes, this loss is the effect of mass transfer limitation at high current densities, and it is readily calculated with expression:

$$\eta_{conc} = \frac{RT_{FC}}{2F}\ln\left(1 - \frac{i}{i_{L,an}}\right) - \frac{RT_{FC}}{4F}\ln\left(1 - \frac{i}{i_{L,ca}}\right) + \frac{RT_{FC}}{2F}\ln(1 + \frac{P_{H2}\ i}{P_{H2O}\ i_{L,an}}) \quad (32)$$

In this expression "F" is faraday's constant, "R" is the universal gas constant, "T_{FC}" is fuel cell operating temperature," $i_{L,an}$" and "$i_{L,ca}$" are limiting current density of anode and cathode respectively and "i" is fuel cell current density.

Fuel cell power produced for FC stack containing "n_{FC}" cells is determined as [29]:

$$\dot{W}_{stack} = n_{FC} \times i \times E(i) \times A_{cell} \quad (33)$$

Here, A_{cell} is the cell area.

2.5. Electric motor

For modeling an electric bus, we use some parameters that were introduced in the vehicle dynamic section. Common parameters in this part include the rolling resistance "C_{RR}", the grade angle of the road (grade angle is accounted by calculation of elevation differences between points of travel), and inertia force which is calculated using vehicle's acceleration. The vehicle parameters in this simulation are frontal area "A_f", drag coefficient "C_d", wheel radius "r", and loaded mass of bus "m". The motor parameters include motor loss constants, "k_i", "k_c", "k_ω" and the final gear drive ratio "G",, the maximum power "P_{Max}" and maximum torque "T_{Max}" [30,31]. The electric motors are assumed to be in-wheel hub synchronous motor and they are modeled with constant torque/rotation speed relation, the storage component is a battery with "C" capacity and auxiliary power demand of ventilation, cooling and heating is counted as "P_{aux}", other electric motor essential simulation properties such as voltage of open battery circuit and its internal resistance are mentioned in table 1.

[DOI: 10.22068/ase.2020.542]

2.6. Life cycle assessment

LCA software is categorized as data record sets of emissions, carbon intensity, and greenhouse gases emitted in the life cycle of a product. In this research total life cycle of a vehicle is considered, which consists of vehicle cycle, operation cycle, and fuel cycle. Vehicle cycle includes material production, vehicle assembly and vehicle disposal; fuel cycle consists of processes of well exploration, oil extraction, refinery, transportation of fuel to fuel station and combustion process. In order to ensure the quality of output data, in this research, two well-known software are used, "GREET" and "GHGenious"[15,16,32].

GREET model uses a comprehensive lifecycle-based approach to compare the energy use and emission spread of conventional and advanced vehicle technologies, for example, hybrid electric vehicles and fuel cell vehicles. Different pathways of each component are available in this software. The criteria for choosing the selected pathways in this research is abundance, and availability of each pathway in the target area. Probable pathway alternatives are considered in this discussion based on its environmental effect and deployment cost.

2.7. General assumptions and specification

For conducting results, it is compulsory to determine some assumptions, so table 1 states all needed data to simulate models used in this research.

Table 1:assumptions and system specifications

Decision parameter	value
Curb mass/Bus full Load	$11380/5100\ \mathrm{kg}$
Frontal area (A)	$8.2\ \mathrm{m}^2$
Center of gravity height	$1.3\ \mathrm{m}$
Transmission efficiency (N_T)	0.96
Differential efficiency (N_{diff})	0.92
Air density (ρ)	$1.22\ \frac{\mathrm{kg}}{\mathrm{m}^3}$
Drag coefficient (C_D)	0.7
Ambient temperature	$298\ \mathrm{k}$
Ambient pressure	$101.325\ \mathrm{kPa}$
Faraday constant (F)	$96485.33\ \mathrm{A/mol}$
Gas constant (R)	$8.314\ \frac{\mathrm{J}}{\mathrm{mol.K}}$
Diesel engine power	$185\ \mathrm{kW}$
Cell area (A_{cell})	$900\ \mathrm{cm}^2$
Cell number (n_{FC})	3×111
Fuel cell temperature (T_{FC})	$343.15\ \mathrm{k}$
Fuel cell pressure	$2\ \mathrm{bar}$
Current density (i)	$1150\ \mathrm{mA/cm}^2$
Fuel cell net power	$3 \times 59\ \mathrm{kW}$
Membrane thickness (L_m)	$0.0183\ \mathrm{cm}$
Cathode limiting current density ($i_{L,cat}$)	$16\ \mathrm{A/cm}^2$
Anode limiting current density ($i_{L,an}$)	$58\ \mathrm{A/cm}^2$
Electric motor max. power	$160\ \mathrm{kW}$
Battery capacity	$240\ \mathrm{kW.h}$
Open circuit voltage	$600\ \mathrm{V}$
Accessory load (HVAC)	$5\ \mathrm{kW}$

3. Results

3.1. Energy demand

For conducting standard and comprehensive results, as mentioned before, four different routes used. Consequently, results contain all aspects of the real driving condition (e.g., unexpected start/stop, road elevation change and the city traffic), in this part besides energy demand calculation in each segment (elevation, inertia, drag and rolling resistance), some specifications of these four routes (e.g., total travel length, travel duration, and average speed) are mentioned (table 2) to give a tangible understanding of routes, to the reader.

To represents energy demand results, it is a customary method to standardize results. This methodology expresses the amount of energy needed to travel one kilometer (kJ/km). To do that, we sum up all the energy demand segments, then divide it by total travel length.

For the first part, the results of real driving cycles are presented according to the route and energy segment. From table 2, it is understood that north and south routes have an average slope of +2.5% and -2.5%, respectively, which is a considerable amount of elevation. As it is expected, these two routes, have considerable

[DOI: 10.22068/ase.2020.542]

elevation energy demand, while east and west routes have venial elevation energy demand.

Table 2: Four routes energy consumption considering different sectors

Routes	Travel length (m)	Travel duration (min)	Average Elevation	ED of elevation (kJ/km)	ED of Drag force (kJ/km)	ED of Rolling resistance (kJ/km)	ED of Acceleration force (kJ/km)
North	11609.7	55	+2.5%	1454.861	129.2117	513.33	1259.521
South	12746.7	61	-2.5%	-1411.09	137.7093	513.2676	1333.1409
East	18002	65	+0.4%	+132.768	136.5686	522.819	901.9275
West	14612.8	75	-0.4%	-164.238	121.7179	465.2829	786.7291

Results presented in Table 2, indicate that the main difference between different routes is mainly in the energy demand of elevation and inertia force. The road slope and travel length are the most effective parameters on these values, and also it can be helpful to mention that rolling resistance and drag force energy losses in all routes are almost the same, and this fact can verify our calculations.

Another critical discussion is about the comparison of the standard and real driving cycles. Results obtained from WLTP cycle and real driving cycle are presented and compared in figure 5, and the figure states each driving cycle energy demand segment separately.

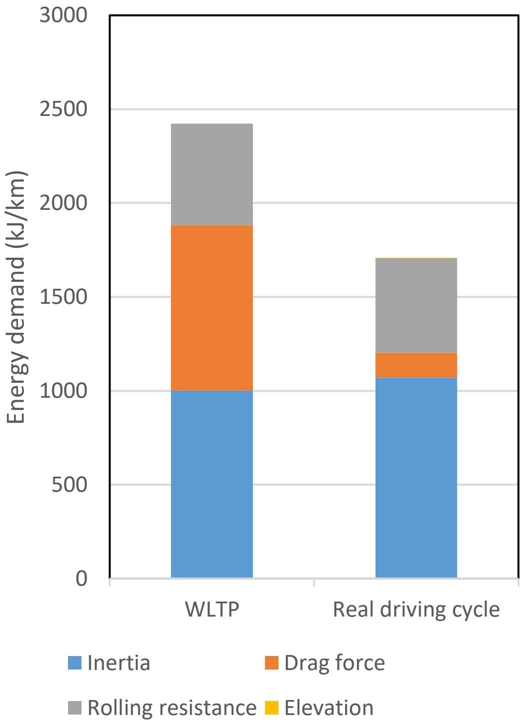

Figure 6:WLTP and real driving cycle energy demand comparison

The main deviation of energy demand between WLTP and the real driving cycle is due to the characteristic of each driving pattern, for instance, WLTP cycle features a higher speed profile than a real driving pattern, and higher average speed causes a higher amount of drag losses in WLTP cycle. On the other hand, numerous stops in city bus driving pattern, cause more inertia energy use in order to supply enough energy for acceleration after each stop, which is evident in figure 6.

3.2. Propulsion systems comparison

[DOI: 10.22068/ase.2020.542]

In this part, efficiency and fuel consumption of buses using different engines (or motor) are calculated. The aforementioned assumptions are employed in this part to simulate internal combustion, fuel cell and electric buses.

3.2.1. Fuel cell bus

For fuel cell buses we obtain the energy demand of each recorded real driving pattern. Then we standardize it by calculating the average amount of energy that is needed for travelling one-kilometer. Afterwards, from the results of previous part (energy demand of each cycle) we distinguish the energy efficiency (first law's efficiency) of this engine type.

In Fig. 7, we observe the effects of different strategies on fuel economy of our real driving cycle. In this figure, we conclude that vehicles have better fuel economy, and consume one kilogram of hydrogen in two kilometer (approximately 14% more) considering the regenerative braking system. Also, if the engine do not have degradation, vehicle will travel three kilometer, with consuming one kilogram of hydrogen more (approximately 21% more) [16].

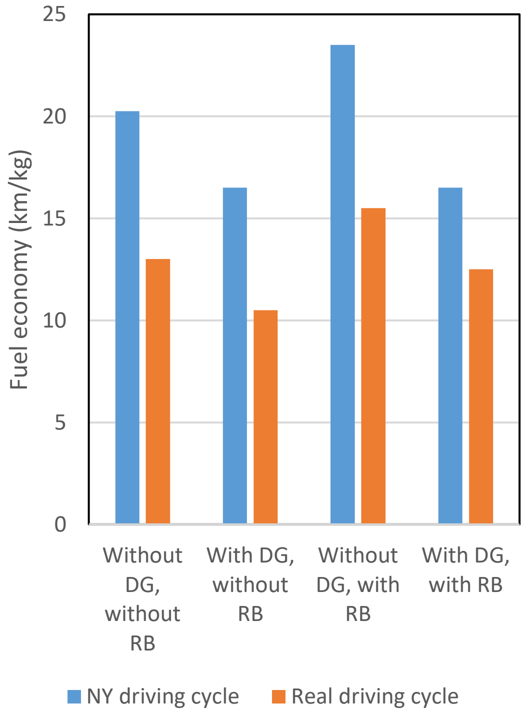

Figure 7:New York and real driving cycles fuel economy considering RB and degradation

3.2.2. Electric bus

According to the electric motor modeling method mentioned before and the research conducted by Misanovi et. al [33], two electric buses simulated, and the results of energy consumption are given as:

Table 3:Electric bus real simulation of energy demand

Bus alternative	Standard energy consumption (kW.h/Km)	Consumed energy	RB energy	Energy of auxiliary devices	Traction energy
BYD E-12(2*90 KW)	1.12	363.4	0	163	200.4
Trolley BKM-321(180 KW)	1.37	440	93	215	225

In this research two electric buses, one of them using regenerative braking and the other one not using this technology, are considered. The results may also vary slightly due to engines efficiencies and arrangements, for instance in BYD-E12 model, two separate electric motors are used which may be the reason of less electricity consumption of this model.

3.2.3. Diesel engine bus

Results for a bus that is powered by internal combustion engine obtained, considering the fact that the IC engine uses diesel fuel ($C_{12}H_{23}$) with first-law efficiency of 35%, also it is necessary to note that power train efficiency and losses due to drag force, rolling resistance and elevation is considered in IC engine simulation. The data for fuel consumption of this bus is presented below:

Table 4:Diesel engine simulation values

Energy consumption	amount
kW.h/km	2.46
L/100km	24.9

3.3. Life cycle assessment

Life cycle assessment measures the impact of a product manufacturing process on the environment, from the materials used to make it to its ultimate disposal. This intention to decide for production of technology or device based on its impact on the environment from different aspects, make this part of research substantial, in this part well to wheel (WTW) stage, and operation stage, or th summation of these two stages, called well to pump (WTP) stage is considered. in addition, vehicle cycle which determines components and devices used for the production of each type of bus is provided separately. Summation of these cycles form total life cycle assessment of the vehicle.

[DOI: 10.22068/ase.2020.542]

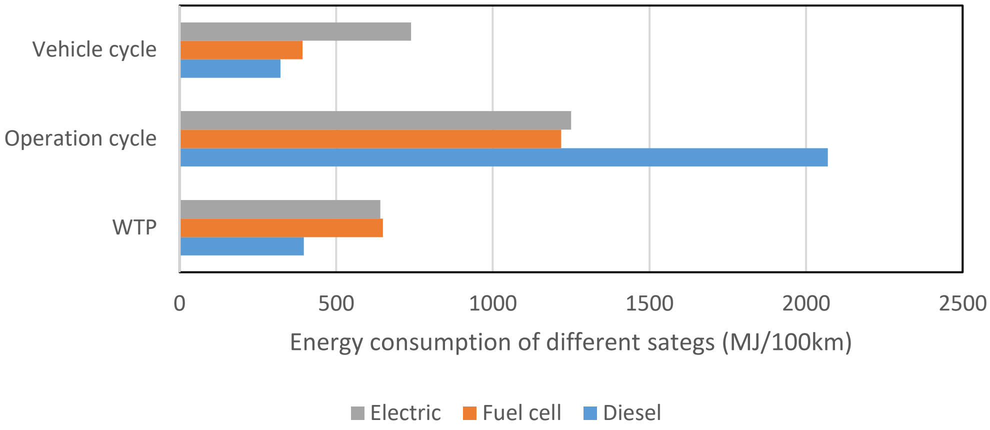

Figure 8:Energy analysis of different stages of the total life cycle

Data given in figure 7 is related to the total life cycle of each bus alternative. As it is understood from the data, in the fuel production process (WLP), buses featuring fuel cell and electric technology consume almost the same amount of energy whereas diesel bus use truly less energy. In operation cycle, which is related to the time the vehicle is being used in the transportation system till disposal, diesel bus consumes more energy than fuel cell and electric buses, in this stage, both electric and fuel cell buses consume almost the same amount of energy. Finally, the vehicle cycle, that includes LCA of components used in each bus alternative, indicate an obvious difference in terms of energy consumption, in this cycle electric buses due to use of high capacity lithium-ion batteries and fuel cell buses for utilizing Ni-MH batteries as temporary energy saving device, use the most amount of energy respectively. At last, conventional diesel engines use the least energy amount in vehicle cycle.

This comparison can be conducted in terms of CO_2 emission production rate, which is presented in figure 9. in the operation stage, undoubtedly electric bus emits the least emission because of not using any combustion or reaction, then the fuel cell buses emit the least amount of emissions, and as we expected, the diesel engine produces the most CO_2 in the operation cycle. For a reliable deduction, total life cycle must be considered, in this case diesel engine is the worst alternative among all choices the reason is huge amount of CO_2 emission produced in operation stage. In terms of other emissions such as CO, SOx, NOx, PM10 and PM2.5 in total life cycle, electric buses emit SO_X, CO and PM10 more than other choices, and diesel engine produces NO_X the most. For PM2.5 emission, all alternatives emit almost the same amount of it, and there is no significant difference between different engines. The statistics of emission production can be seen schematically in figure 9.

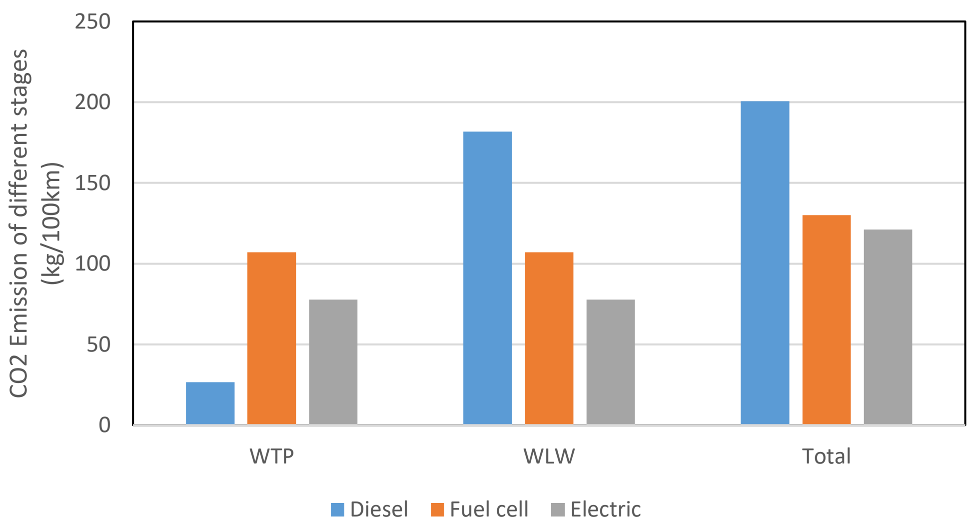

Figure 9:CO2 Emitted for bus alternatives in different stage

[DOI: 10.22068/ase.2020.542]

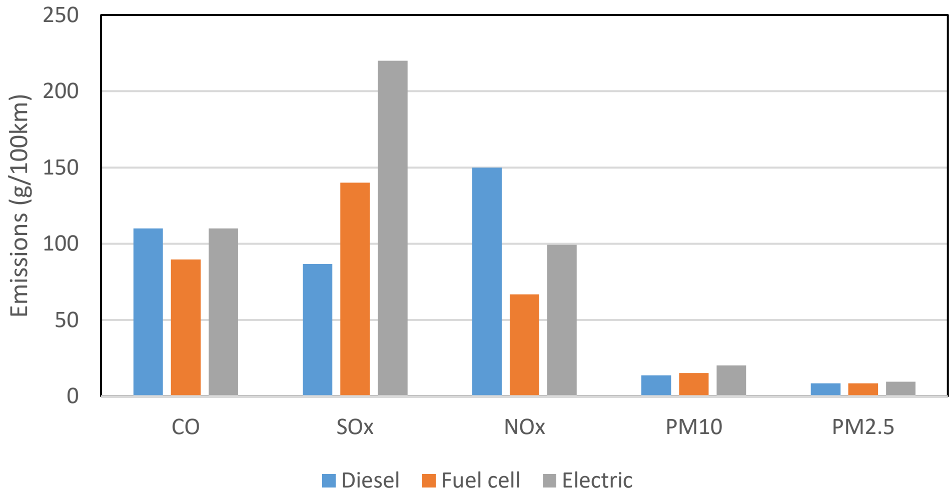

Figure 10: Five different emissions emitted by bus alternatives

To evaluate and compare different bus alternatives in terms of LCA, it is good to focus on each engine type separately, next three figures give extensive information about each one, and says in detail that which process (producing vehicle components, fluids, batteries, operation or fuel cycle) has how much share in each emission release or energy consumption. for example, fuel cell bus is considered to be emission producing, mostly in the fuel cycle, and in case of energy consumption, it is operation stage that has the most significant portion. For electric buses we can see the same trend as fuel cell buses but diesel buses produce most of the emission in the operation stage; besides that, this stage has a pivotal role in total life cycle energy usage too.

.

[DOI: 10.22068/ase.2020.542]

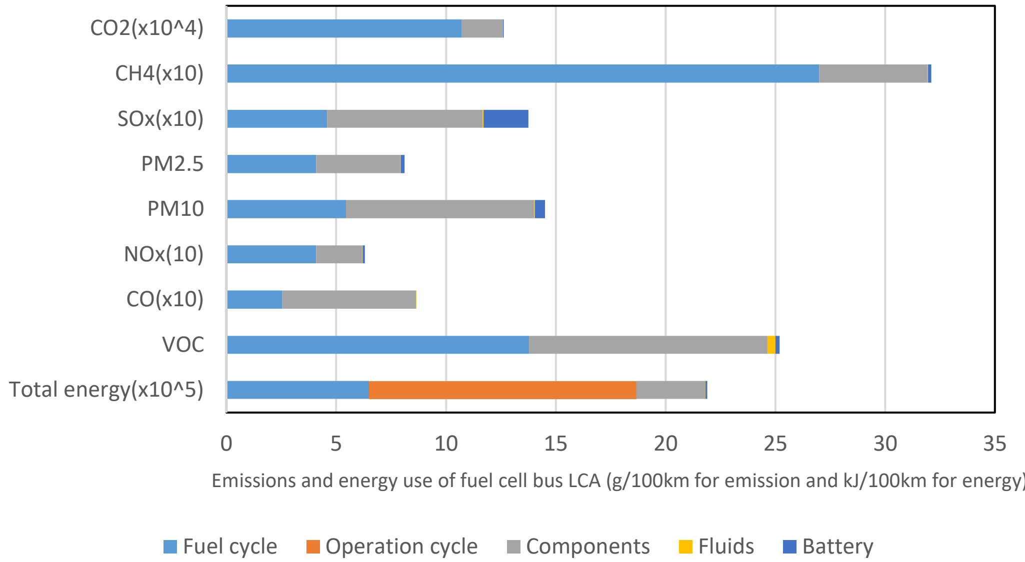

Figure 11:Emission and energy consumed of fuel cell bus cycle

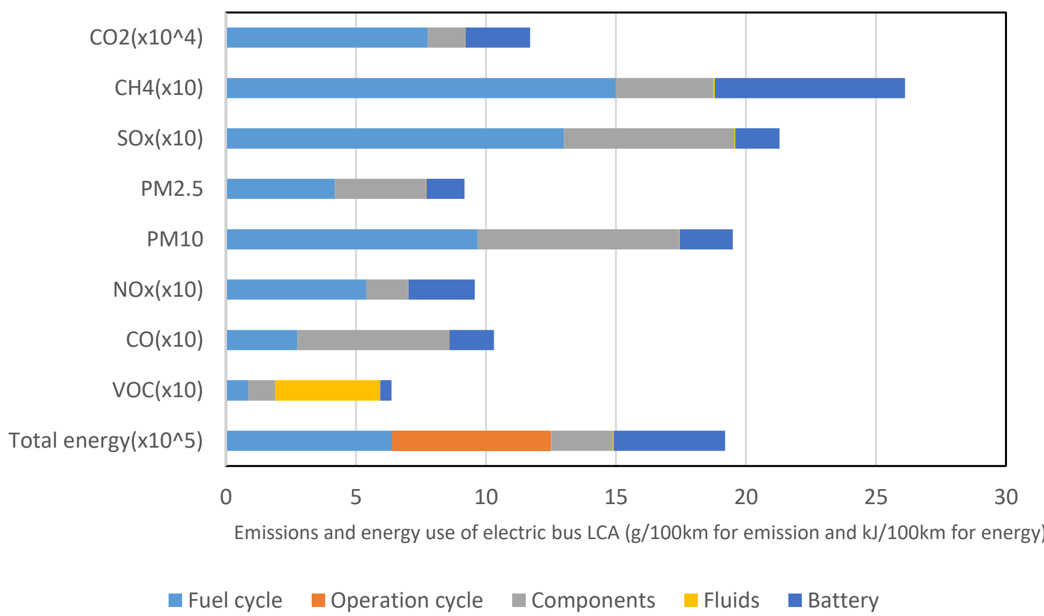

Figure 12:Emission and energy consumed of electric bus cycle

[DOI: 10.22068/ase.2020.542]

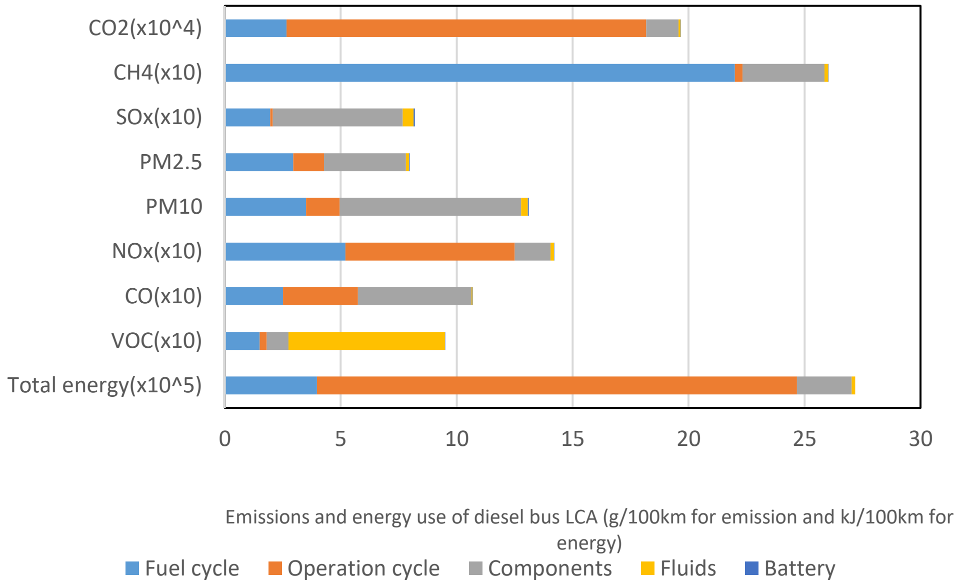

Figure 13:Emission and energy consumed of diesel bus cycle

3. Discussion

What mentioned and discussed in results consist of energy demand calculation based on real and standard driving cycles, different bus alternatives simulated and their fuel or electricity consumption obtained. Finally, LCA analysis for target buses conducted. To verify our results in this part, the efficiency of each instance is calculated, these results can be compared to submitted manuscripts. These calculations are done just for real driving patterns.

For simulated diesel IC engine and electric bus we calculated $4.42\, kW.h/km$ and $1.12\, kW.h/km$ energy usage respectively, this computation for fuel cell buses conducted and four strategies were considered here we assume to have degradation and no regenerative braking for considered alternative, the fuel consumption for this choice is $10.5 \frac{km}{kg\ H_2}$, By noting hydrogen Lower heating value ($119\ MJ/kg$) we obtain $3.14\, kW.h/km$ for the fuel cell bus.

Back to the energy demand section, for real driving cycles, the average amount of energy demand calculated about $0.49\, kW.h/km$, which yield to efficiency results below.

$$\eta_{ICE} = \frac{0.49}{(2.46 - 0.4)} = 23.8\%$$

$$\eta_{FC} = \frac{0.49}{(1.79 - 0.4)} = 35.5\%$$

$$\eta_{electric} = \frac{0.49}{(1.24 - 0.4)} = 58.3\%$$

This calculation presents a generalized understanding of the huge amount of energy loss in FC and ICE buses, another important point is the environmental effect of vehicle cycle, as said in LCA part, producing components related to batteries (especially high capacity lithium-ion batteries) which are widely used in electric vehicles has much more side effects than other two alternatives, so considering all aspects of this issue, it seems the best to put our effort on using optimized FC or ICE engines till achieving less harmful manufacturing methods of producing lithium-ion or using its more environmentally friendly substitutes.

4. Conclusions

This paper examines buses utilizing three different power sources, for each case we

[DOI: 10.22068/ase.2020.542]

derived fuel consumption and LCA analysis, more over the energy demand is calculated using real and standard driving cycles, real driving cycles are acquired from inner-city buses which face many starts and stops, due to that the energy demand of different sections may vary in comparison to standard driving cycles, for instance, inertia energy use in a real driving pattern is more than standard driving cycle, while energy use of rolling resistance and drag force is considerably less, this difference appears because of higher average velocity in WLTP cycle and other differences in each driving pattern characteristic.

The research concluded that in terms of energy, electric, fuel cell and diesel IC buses are the most efficient fleet respectively.

To consider each substitute advantages and disadvantages from another point of view, LCA analysis performed next. Results showed that although electric buses were the most efficient, and they had the least amount of energy loss in operation cycle, but in the manufacturing process they are more devastative by consuming almost twice energy than other alternatives. However they consume energy in total life cycle with just 5% dfference than fuel cell and diesel buses. Concerning CO_2 emission, diesel IC buses emit 201 (kg/100km) which almost 85% of this emission is produced in operation stage, for fuel cell buses that totally emit 130 (kg/100km), the well to pump stage portion is about 82% and in operation stage no CO_2 is emitted. Finally electric buses produce 78 (kg/100km) in well to pump stage and 121 (kg/100km) totally. As a result, it is understood from the results that although conventional diesel engine buses have economic justification, they emit the most emissions, which brings a superficial disadvantage for this kind of economic bus fleet.

List of symbols

A	**Vehicle frontal area**
A_{cell}	Cell area
a_x	Acceleration
C_D	Drag coefficient
D_A	Drag force
E_{rr}	Energy of rolling resistance
$E(i)$	Fuel cell voltage
F_x	Force of acceleration
F_{trac}	Traction force
F_{grade}	Elevation force
F_{roll} or F_{RR}	Rolling resistance force
i	Current density
$i_{L,cat}$	Cathode limiting current density
$i_{L,an}$	Anode limiting current density
I_d	Drive train inertia
I_w	Wheel inertia
I_t	Transmission inertia
L_m	Membrane thickness
M	Mass of vehicle
M_r	Equivalence mass of rotating parts
N_T	Transmission ratio
N_{diff}	Differential ratio
$N_{T,diff}$	Transmission and differential ratio
n_{FC}	Cell number
P_{FC}	Fuel cell pressure
R_x	Rolling resistance force
R_{hx}	Carrier force

r	Tire radius
$\boldsymbol{T_a}$	Axle torque
$\boldsymbol{T_c}$	Clutch torque
$\boldsymbol{T_e}$	Engine torque
$\boldsymbol{T_{FC}}$	Fuel cell temperature
V	Speed
$\boldsymbol{\alpha}$	Angular velocity
$\boldsymbol{a_w}$	Angular velocity of wheel
$\boldsymbol{\rho}$	Air density
$\boldsymbol{\eta_{T,diff}}$	Transmission and differential efficiency
$\boldsymbol{\lambda_{air}}$	Air stochiometric ratio

References

[1] Suganthi L, Samuel AA. Energy models for demand forecasting - A review. Renew Sustain Energy Rev 2012. doi:10.1016/j.rser.2011.08.014.

[2] Ahmadi P. Environmental impacts and behavioral drivers of deep decarbonization for transportation through electric vehicles. J Clean Prod 2019. doi:10.1016/j.jclepro.2019.03.334.

[3] Ahmadi P, Cai XM, Khanna M. Multicriterion optimal electric drive vehicle selection based on lifecycle emission and lifecycle cost. Int J Energy Res 2018. doi:10.1002/er.3937.

[4] Lajunen A. Energy consumption and cost-benefit analysis of hybrid and electric city buses. Transp Res Part C Emerg Technol 2014;38:1–15. doi:10.1016/j.trc.2013.10.008.

[5] Vepsäläinen J, Otto K, Lajunen A, Tammi K. Computationally efficient model for energy demand prediction of electric city bus in varying operating conditions. Energy 2019;169:433–43. doi:10.1016/j.energy.2018.12.064.

[6] Gallet M, Massier T, Hamacher T. Estimation of the energy demand of electric buses based on real-world data for large-scale public transport networks. Appl Energy 2018;230:344–56. doi:10.1016/j.apenergy.2018.08.086.

[7] Cubito C, Millo F, Boccardo G, Di Pierro G, Ciuffo B, Fontaras G, et al. Impact of different driving cycles and operating conditions on CO2 emissions and energy management strategies of a Euro-6 hybrid electric vehicle. Energies 2017;10. doi:10.3390/en10101590.

[8] Ahmadi P, Kjeang E. Comparative life cycle assessment of hydrogen fuel cell passenger vehicles in different Canadian provinces. Int J Hydrogen Energy 2015. doi:10.1016/j.ijhydene.2015.07.147.

[9] Ahmadi P, Kjeang E. Realistic simulation of fuel economy and life cycle metrics for hydrogen fuel cell vehicles. Int J Energy Res 2017. doi:10.1002/er.3672.

[10] Changizian S, Ahmadi P, Raeesi M, Javani N. Performance optimization of hybrid hydrogen fuel cell-electric vehicles in real driving cycles. Int J Hydrogen Energy 2020. doi:10.1016/j.ijhydene.2020.01.015.

[11] Gao D, Jin Z, Lu Q. Energy management strategy based on fuzzy logic for a fuel cell hybrid bus. J Power Sources 2008;185:311–7. doi:10.1016/j.jpowsour.2008.06.083.

[12] Fontaras G, Karavalakis G, Kousoulidou M, Tzamkiozis T, Ntziachristos L, Bakeas E, et al. Effects of biodiesel on passenger car fuel consumption, regulated and non-regulated pollutant emissions over legislated and real-world driving cycles. Fuel 2009;88:1608–17. doi:10.1016/j.fuel.2009.02.011.

[13] Jonker G, Harmsen J. Creating Design Solutions. Eng Sustain 2012:61–81.

doi:10.1016/b978-0-444-53846-8.00004-4.

[14] Correa G, Muñoz PM, Rodriguez CR. A comparative energy and environmental analysis of a diesel, hybrid, hydrogen and electric urban bus. Energy 2019;187. doi:10.1016/j.energy.2019.115906.

[15] Ally J, Pryor T. Life-cycle assessment of diesel, natural gas and hydrogen fuel cell bus transportation systems. J Power Sources 2007;170:401–11. doi:10.1016/j.jpowsour.2007.04.036.

[16] Ahmadi P, Torabi SH, Afsaneh H, Sadegheih Y, Ganjehsarabi H, Ashjaee M. The effects of driving patterns and PEM fuel cell degradation on the lifecycle assessment of hydrogen fuel cell vehicles. Int J Hydrogen Energy 2020;45:3595–608. doi:10.1016/j.ijhydene.2019.01.165.

[17] Granovskii M, Dincer I, Rosen MA. Life cycle assessment of hydrogen fuel cell and gasoline vehicles. Int J Hydrogen Energy 2006;31:337–52. doi:10.1016/j.ijhydene.2005.10.004.

[18] Samuel S, Morrey D, Fowkes M, Taylor DHC, Austin L, Felstead T, et al. Real-world fuel economy and emission levels of a typical EURO-IV passenger vehicle. Proc Inst Mech Eng Part D J Automob Eng 2005;219:833–42. doi:10.1243/095440705X28277.

[19] Abe M. Fundamentals of Vehicle Dynamics. Veh. Handl. Dyn., 2015, p. 45–107. doi:10.1016/B978-0-08-100390-9.00003-8.

[20] Tsolakis A, Bogarra M, Herreros J. Road Vehicle Technologies and Fuels. Issues Environ Sci Technol 2017:1–24. doi:10.1039/9781788010221-00001.

[21] IEA. CO2 EMISSIONS FROM FUEL COMBUSTION Highlights. Iea 2015. doi:10.1787/co2-table-2011-1-en.

[22] Al-Baghdadi MARS. Modelling of proton exchange membrane fuel cell performance based on semi-empirical equations. Renew Energy 2005;30:1587–99. doi:10.1016/j.renene.2004.11.015.

[23] Wang Y, Chen KS, Mishler J, Cho SC, Adroher XC. A review of polymer electrolyte membrane fuel cells: Technology, applications, and needs on fundamental research. Appl Energy 2011. doi:10.1016/j.apenergy.2010.09.030.

[24] Mert SO, Özçelik Z, Özçelik Y, Dinçer I. Multi-objective optimization of a vehicular PEM fuel cell system. Appl Therm Eng 2011. doi:10.1016/j.applthermaleng.2011.04.031.

[25] Ezzat MF, Dincer I. Comparative assessments of two integrated systems with/without fuel cells utilizing liquefied ammonia as a fuel for vehicular applications. Int J Hydrogen Energy 2018. doi:10.1016/j.ijhydene.2017.07.203.

[26] Ezzat MF, Dincer I. Development and exergetic assessment of a new hybrid vehicle incorporating gas turbine as powering option. Energy 2019. doi:10.1016/j.energy.2018.12.141.

[27] Ezzat M, Dincer I. Exergoeconomic analysis and optimization of a new hybrid fuel cell vehicle. Int J Hydrogen Energy 2020;45:5734–44. doi:10.1016/j.ijhydene.2019.07.104.

[28] Miansari M, Sedighi K, Amidpour M, Alizadeh E, Miansari M. Experimental and thermodynamic approach on proton exchange membrane fuel cell performance. J Power Sources 2009;190:356–61. doi:10.1016/j.jpowsour.2009.01.082.

[29] Ezzat MF, Dincer I. Development and assessment of a new hybrid vehicle with ammonia and hydrogen. Appl Energy 2018. doi:10.1016/j.apenergy.2018.03.012.

[30] Czogalla O, Jumar U. Design and control of electric bus vehicle model for estimation of energy consumption. IFAC-PapersOnLine 2019;52:59–64.

doi:10.1016/j.ifacol.2019.12.381.

[31] Xiong W, Zhang Y, Yin C. Optimal energy management for a series-parallel hybrid electric bus. Energy Convers Manag 2009;50:1730–8. doi:10.1016/j.enconman.2009.03.015.

[32] Wang MQ, Contact P. XI . 2 Life-Cycle Analysis of Vehicle and Fuel Systems with the GREET Model 2015:15–8.

[33] Mišanoví SM, ŽIvanović ZM, Tica SM. Energy efficiency of different bus subsystems in Belgrade public transport. Therm Sci 2015;19:2233–44. doi:10.2298/TSCI151116193M.